Pergamon

Int. J. Heat Mass Transfer. Vol. 40, No. 11, pp. 2709–2719, 1997

Printed in Great Britain
0017–9310/97 $17.00+0.00

PII: S0017-9310(96)00232-3

Conjugate heat transfer from a small heated strip

K. D. COLE

Mechanical Engineering Department, 255 Walter Scott Engineering Center, University of Nebraska-Lincoln, Lincoln, NE 68588-0656, U.S.A.

(*Received* 4 *January* 1996 *and in final form* 17 *June* 1996)

Abstract—This study addresses the electronic cooling problem from the perspective of scaling laws applied to a simple conjugate heat transfer geometry, steady shear flow over a heated strip on a flat plate. The results are reported in a compact form in terms of a modified Nusselt number and a combined parameter $(k_f/k_s)Pe^{1/3}$. Numerical results are reported that apply to a wide range of values for fluid flow, thermal conductivity, and thickness of the flat plate, and the results include simple design correlations. A new dimensionless parameter is suggested for determining when the fluid axial heat conduction can be neglected.

1. INTRODUCTION

In 1961 Perelman [1] coined the phrase 'conjugated heat transfer' to describe the heat transfer between a fluid and a solid in which the interface condition is initially unknown and is found from the heat transfer solution. In the past three decades there has been much research in this area with applications including aerodynamic heating, high-efficiency heat exchangers, hot-film sensors, and electronic cooling. Recently there has been strong interest in electronic cooling applications, however some of this work has not taken advantage of dimensionless parameters identified in the conjugate heat transfer literature. This study approaches the electronic cooling problem from the perspective of conjugate heat transfer to take advantage of the scaling laws and dimensionless parameters appropriate to a simple geometry, steady flow over a heated strip on a flat plate.

A brief review of some conjugate heat transfer literature pertinent to the electronic cooling application is discussed below. The literature discussed below contains one or more of the following elements: use of a combined parameter for presenting the results; theory based on integral equations with temperature matching on the fluid/solid interface; design correlations or approximate formulas.

Perelman [1] studied laminar flow over an internally heated flat plate with asymptotic expansions. Perelman identified a parameter that combined conductivity ratio, Prandtl number and Reynolds number. Luikov [2] used the same combined parameter which he calls the Brun number in an approximate analysis involving a simplified thin–solid geometry with a linear temperature distribution across the solid. Later in this paper the Brun number will be discussed in some detail. Several other researchers have presented results with a combined parameter: Sparrow and Chyu [3] in a finite-difference study of a thin rectangular fin; Wijeysundera [4] in a laminar duct flow with axial wall conduction; Cole and Beck [5] in steady flow with transient heating from a small strip; Lee and Ju [6] in a parallel plate geometry in which the entire plate is heated; Rizk *et al.* [7] with a uniform velocity distribution (slug flow); Pozzi and Lupo [8] with the geometry of Luikov extended to compressible flow; Pop and Ingham [9] also with the geometry of Luikov in which the combined parameter appears as part of the length scale used to normalize the equations.

Many different numerical and analytical methods have been applied to conjugate heat transfer. The present work involves integral equations with temperature and heat flux matching along the interface; these methods have been used for several years [10–14]. Anderson [15] used a summation of discrete elements and an adiabatic heat transfer coefficient for superposition along the fluid–solid interface, however this approach is equivalent to the continuous integrals and Green's functions used in the present research, since the adiabatic heat transfer coefficient is proportional to the reciprocal of the fluid-side Green's function.

Several researchers have studied a range of flow conditions and have presented design correlations of their results: Ramadhyani *et al.* [16] in a finite-difference study of two heat sources on a thick solid; Incropera *et al.* [17] in a combined experimental and theoretical study of a constant temperature copper block flush-mounted in a channel flow; Pozzi and Lupo [8] with viscous dissipation in the compressible flow; and, Prasad and Dey Sarkar [18]. None of these investigators have studied variations in the thickness of the solid.

NOMENCLATURE

a	half-length of heated strip [m]
Br_x	Brun number, equation (15)
C_{fx}	local skin friction coefficient
D	thickness of solid [m]
G	Green's function, equation (16)
k	thermal conductivity [W (m K)$^{-1}$]
M	number of surface elements
N_u	$=h(2a)/k_f$, Nusselt number
N_u^*	$=h(2a)/k_s$, modified Nusselt number
$p(x)$	$=1$ on heated strip $=0$ elsewhere
Pe	$=\beta a^2/\alpha_f$, Peclet number
Pr	Prandlt number
Re	Reynolds number
q	interface heat flux [W m^{-2}]
q_0	source heat flux [W m^{-2}]
T	temperature [K]
x	streamwise coordinate [m]
y	transverse coordinate [m].

Greek symbols

α_f	fluid thermal diffusivity [m^2 s^{-1}]
β	velocity gradient at wall [s^{-1}]
Λ	$=(k_f/k_s)Pe^{1/3}$, conjugate Peclet number
ϕ	influence function, integral of Green's function
ξ	source location, equation (16) [m].

Subscripts

f	fluid
s	solid
i	index for temperature location
j	index for surface element location
∞	ambient.

Superscripts

$(\ )^+$	dimensionless parameters, equation (7)
$\overline{(\ )}$	spatial average on the heated strip.

Sugavanam *et al.* [19] carried out a finite-difference study of a flush-mounted heat source on a circuit board with laminar air flow over one or both sides of the circuit board. Ortega [20] extended this work to include rectangular heat sources and three-dimensional analysis. Both authors studied three discrete values of the board thickness, and they did not include the effect of board thickness in their correlations for Nusselt number.

There are very few experiments reported in a form that allow comparison with theory. Liu *et al.* [21] measured the surface temperature on a small heated strip cooled by air flow with a fluorescent paint technique. Ortega *et al.* [22] carried out an a benchmark experiment with air cooling of a heat source on plexiglas and reported spatial average heat transfer coefficients.

The purpose of the paper is threefold: firstly, to present numerical results for a wide range of fluid flow, thermal conductivity ratio, and solid thickness in terms of a combined parameter $(k_f/k_s)Pe^{1/3}$ called the conjugate Peclet number; secondly, to investigate the limiting behavior for large and small values of the conjugate Peclet number; and thirdly, to suggest a new dimensionless parameter for determining when the fluid axial heat conduction can be neglected in conjugate heat transfer.

2. ANALYSIS

The geometry is shown in Fig. 1. A flat plate contains an embedded heated strip of streamwise length $2a$. The flat plate is composed of a single layer with an effective thickness, D, which may represent a plate composed of several layers (for example an electronic circuit board). The flat plate is cooled by a fluid flow that has a linear velocity profile ($u=\beta y_f$), which is appropriate if the thermal boundary layer caused by the heated region is not too thick and if the local shear stress is not varying too rapidly in the streamwise direction. The thermal properties are constant (small temperature rise assumed). Radiation and natural convection are neglected, axial heat conduction in the fluid is neglected, and viscous dissipation is not present in the fluid.

The equations governing the temperature are given by

$$\text{Fluid} \quad \beta y_f \frac{\partial T_f}{\partial x} = \alpha_f \frac{\partial^2 T_f}{\partial (y_f)^2}; \quad \begin{cases} -\infty < x < \infty \\ 0 < y_f < \infty \end{cases} \tag{1}$$

$$\text{Solid} \quad \frac{\partial^2 T_s}{\partial x^2} + \frac{\partial^2 T_s}{\partial (y_s)^2} = 0; \quad \begin{cases} -\infty < x < \infty \\ 0 < y_s < D \end{cases} \tag{2}$$

with boundary conditions

$$T(x \to -\infty, y) = T(x \to \infty, y) = T_f(x, y \to \infty) = T_\infty \tag{3}$$

$$\frac{\partial T_s}{\partial y_s}(x, D) = 0. \tag{4}$$

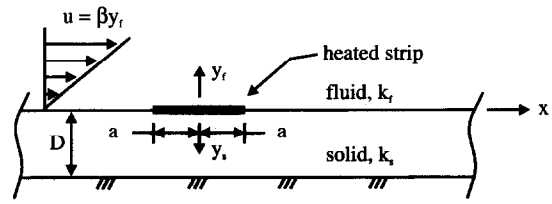

Fig. 1. Conjugate heat transfer geometry.

For perfect thermal contact between the fluid, the surface of the solid and the thin heated strip, the matching conditions are given by

$$T_f(x,0) = T_s(x,0) \tag{5}$$

$$-k_f\frac{\partial T_f}{\partial y_f}(x,0) - k_s\frac{\partial T_s}{\partial y_s}(x,0) = q_0 p(x). \tag{6}$$

Here q_0 is the heat flux introduced by the thin heater and function $p(x)$ is a top-hat function equal to unity on $-a < x < a$ and equal to zero elsewhere.

Next dimensionless variables will be introduced to reduce the number of parameters needed to describe the temperature:

$$x^+ = \frac{x}{a}, y_s^+ = \frac{y_s}{a}, y_f^+ = \frac{y_f}{a}\cdot\left(\frac{\beta a^2}{\alpha_f}\right)^{1/3}, D^+ = \frac{D}{a}$$

$$T_s^+ = \frac{T_s - T_\infty}{(q_0 a/k_s)}, \quad T_f^+ = \frac{T_f - T_\infty}{(q_0 a/k_s)}$$

$$q_s^+ = -\frac{k_s}{q_0}\frac{\partial T_s}{\partial y}\bigg|_{y=0}, \quad q_f^+ = -\frac{k_f}{q_0}\frac{\partial T_f}{\partial y}\bigg|_{y=0}. \tag{7}$$

The length scale is chosen to be 'a', the half-length of the heated strip, which is useful when the fluid convective heat transfer is the dominant mechanism. Later in the paper parameters based on length scale 'D' will also be used. With the above parameters, equations (1) and (2) can be expressed in dimensionless form:

$$\text{Fluid} \quad y_f^+\frac{\partial T_f^+}{\partial x^+} = \frac{\partial^2 T_f^+}{\partial (y_f^+)^2}; \quad \begin{cases} -\infty < x^+ < \infty \\ 0 < y_f^+ < \infty \end{cases} \tag{8}$$

$$\text{Solid} \quad \frac{\partial^2 T_s^+}{\partial (x^+)^2} + \frac{\partial^2 T_s^+}{\partial (y_s^+)^2} = 0; \quad \begin{cases} -\infty < x^+ < \infty \\ 0 < y_s^+ < D/a \end{cases} \tag{9}$$

The boundary conditions in dimensionless form are especially identical to equations (3) and (4) and will not be repeated. The dimensionless matching conditions are given by

$$T_f^+(x^+,0) = T_s^+(x^+,0) \tag{10}$$

$$-\Lambda\frac{\partial T_f^+}{\partial y_f^+}(x^+,0) - \frac{\partial T_s^+}{\partial y_s^+}(x^+,0) = p(x^+) \tag{11}$$

where $\Lambda = (k_f/k_s)\ (\beta a^2/\alpha_f)^{1/3}$ is called the conjugate Peclet number in which βa is the characteristic velocity.

The dimensionless boundary value problem given above indicates that the temperature depends on coordinates x^+ and y^+, on the conjugate Peclet number Λ, and on the geometry D^+. That is, the functional form of the temperature can be expressed as $T_f^+ = T_f^+(x^+, y_f^+, \Lambda, D^+)$ for the fluid side and a similar relationship can be written for the solid side. This important result, reported previously [6, 23] indicates that a short list of parameters embodies all aspects of the temperature in the conjugate heat transfer problem, including the fluid flow, the thermal properties, and the geometry of the solid. The temperature on the interface at $y = 0$ has the functional relationship $T^+ = T^+(x^+, \Lambda, D^+)$ and finally the spatial average temperature on the heated region has the functional form $\overline{T^+} = \overline{T^+}(\Lambda, D^+)$ where the overbar is used to denote a spatial average.

2.1. *Nusselt number*

The Nusselt number N_u is often used in conjugate heat transfer to present results in dimensionless form even though N_u is a derived parameter, not a fundamental parameter, since N_u does not appear in equations (8)–(11). Let the spatial-average Nusselt number be defined as

$$\overline{N_u} \equiv \overline{\left(-k_f\frac{\partial T_f}{\partial y_f}\frac{1}{(T_f - T_\infty)}\right)_{y_f=0}}\frac{2a}{k_f} \tag{12}$$

where the expression in brackets is the average heat transfer coefficient on the heated region of the fluid–solid interface and where the length scale is $2a$, the streamwise length of the heated region. Using the dimensionless parameters given in equation (7), the Nusselt number may be stated in the form

$$\overline{N_u} = 2P_e^{1/3}\overline{\left(\frac{\partial T_f^+}{\partial y_f^+}\frac{1}{T_f^+}\right)}\bigg|_{y_f^+=0}. \tag{13}$$

Since dimensionless temperature T_f^+ depends on parameters Λ and D/a, the above expression shows that the functional form of the spatial-average Nusselt number can be stated $\overline{N_u} = \overline{N_u}(\Lambda, D/a, Pe)$ where $Pe = \beta a^2/\alpha_f$ is the (local) Peclet number. Lee and Ju [6] showed that a modified Nusselt number defined by $\overline{N_u^*} \equiv (k_f/k_s)\overline{N_u}$ is a more appropriate parameter because its functional form has fewer dimensionless parameters; that is, $\overline{N_u^*} = \overline{N_u^*}(\Lambda, D/a)$. This result can be derived by multiplying equation (13) by (k_f/k_s) to obtain:

$$\overline{N_u^*} = 2\Lambda\overline{\left(\frac{\partial T_f^+}{\partial y_f^+}\frac{1}{T_f^+}\right)}\bigg|_{y_f^+=0}. \tag{14}$$

Parameter $\overline{N_u^*}$ has important implications for the compact presentation of experimental data and on the creation of the useful design correlations for conjugate heat transfer. For example, experiments carried out for one solid material (such as one type of circuit board in an electronic cooling application) may be used to predict the heat transfer results for a variety of solid materials.

2.2. *Brun number*

In this section the Brun number discussed by Luikov [2] is related to the conjugate Peclet number. Luikov studied a finite-length flat plate with constant temperature on the bottom side of the plate and convection on the top side. Luikov introduced the Brun

number with a scaling argument based on the wall flux matching condition, equation (6), in discrete form

$$-k_s \frac{\Delta T_s}{D}\bigg|_{y_s=0} - k_f \frac{\Delta T_f}{\delta_f}\bigg|_{y_f=0} = 0$$

(note the absence of a heated strip) where δ_f is the thickness of the thermal boundary layer in the fluid. The value δ_f may be estimated from a fluid-only Nusselt number correlation according to $\delta_f(x) \sim x/N_{ux}$ where for an isothermal plate $N_{ux} = A \cdot (Pr)^m (Re_x)^m$ (here 'A' is some constant). Combine all these relations into the above flux matching condition and solve for the ratio of the temperature differences. The Brun number is taken to be proportional to the temperature ratio, given by

$$\frac{\Delta T_s}{\Delta T_f} \sim Br_x = \frac{D}{x}\frac{k_f}{k_s} \cdot (Pr)^m (Re_x)^m. \tag{15}$$

Luikov used the Brun number Br_x as the criterion for determining when conjugate analysis should supplant fluid-only analysis for the finite-plate geometry; if the Brun number is large enough then conjugate analysis is required.

The conjugate Peclet number used in the present research, $\Lambda = (k_f/k_s)\,(Pe)^{1/3}$, although derived from the dimensional analysis of equations (1)–(6), is related to the Brun number in the particular case of shear flow. If the velocity profile is linear, and further if the velocity profile varies slowly in the streamwise direction, then the fluid-only correlation for the Nusselt number on an isothermal plate is $N_{ux} = A \cdot (Pr)^{1/3} (Re_x)^{1/3}$. In this case the Brun number becomes

$$Br_x = \frac{D}{x}\frac{k_f}{k_s} \cdot (Pr \cdot Re_x)^{1/3}$$

which actually contains the conjugate Peclet number. This Brun number would be appropriate for shear flow over a finite-length flat plate with a constant temperature imposed at the bottom of the plate.

2.3. *Surface element method*

The numerical results presented in this paper were obtained with the surface element (SE) method, a variant of the boundary element (BE) method, and a brief discussion of the numerical method is presented below. The temperature in each body may be stated as an integral of an unknown heat flux distribution and a known Green's function,

$$T_s^+(x, y=0) = \int_{-\infty}^{\infty} q_s^+(\xi) G_s(x-\xi)\, d\xi^+$$

$$T_f^+(x, y=0) = \frac{k_s}{k_f}\int_{-\infty}^{\infty} q_f^+(\xi) G_f(x-\xi)\, d\xi^+. \tag{16}$$

The Green's function $G(x-\xi)$ is the dimensionless temperature rise at position x in each body (fluid or solid) due to an infinitesimal heat source located at position ξ on the $y = 0$ interface. The Green's functions are found using well-known methods [24]. The Green's function integral for each body is transformed into a linear algebraic equation by discretizing the interface between the fluid and the solid into M surface elements, and by taking the heat flux to be piecewise constant over each surface element. Then, the Green's function integral for each body is written in discrete form:

$$T_s^+(x_i, 0) = \sum_{j=1}^{M} \phi_s(x_i, x_j) q_s^+(x_j)$$

$$T_f^+(x_i, 0) = \sum_{j=1}^{M} \phi_f(x_i, x_j) q_f^+(x_j). \tag{17}$$

Influence functions ϕ are integrals of the Green's functions that represent the (dimensionless) temperature rise at location x_i caused by a unit heat flux over a surface element centered at location x_j. Because the influence functions for the SE method depend on the type of boundary conditions in each body, only that subset of the fluid–solid interface that is actively transferring heat must be discretized. In contrast, the BE method requires that the entire domain boundary be discretized which requires many more elements. In the present work the fluid is semi-infinite and the solid is an infinite slab extending over $(-\infty < x < \infty)$.

The temperatures given by equation (17) may be set equal to one another according to equation (10), and the heat flux to the solid q_s can be eliminated with the heat flux matching condition, equation (11), to give

$$\sum_{j=1}^{M} \phi_f(x_i, x_j) q_f^+(x_j) = \sum_{j=1}^{M} \phi_s(x_i, x_j)(p_j - q_f^+(x_j)).$$

The form appropriate for matrix solution is

$$\sum_{j=1}^{M} [\phi_f(x_i, x_j) + \phi_s(x_i, x_j)] q_f^+(x_j) = \sum_{j=1}^{M} \phi_s(x_i, x_j) p_j. \tag{18}$$

The above expression is a set of M linear algebraic equations for the M unknown heat flux values $q_f^+(x_j)$. Once the heat fluxes have been found, then the temperature T^+ and the Nusselt number may be calculated anywhere on the fluid–solid interface. Typically $M = 32$ variable-length surface elements are needed (eight on the heated region) to adequately describe the spatial average heat flux and Nusselt number; additional refinement changes the spatial average results less than 0.1%. Calculation of the heat flux and temperature distribution for one geometry at $M = 32$ requires about 0.6 CPU seconds on a DEC AlphaAXP 2100 computer.

The numerical results of this method have been verified by comparison with literature calculations that involve the fully-developed linear velocity distribution. The results have also been checked against the conjugate calculations of Sugavanam *et al.* [19] in which a heated strip is located in the laminar entrance

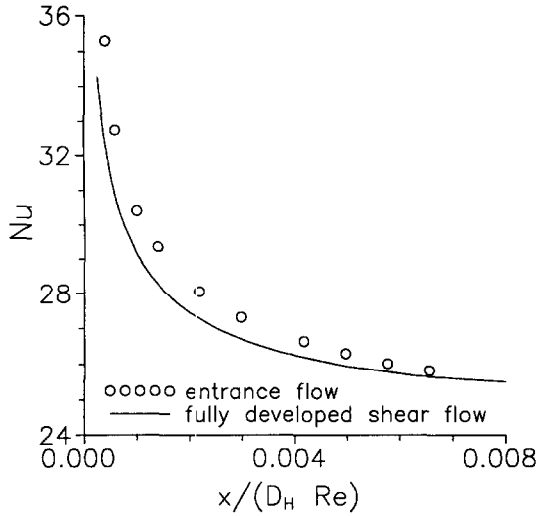

Fig. 2. Spatial average Nusselt number on the heat source vs distance for laminar entrance flow [19] and for fully developed shear flow with matching local shear stress.

region of a parallel-plate flow. To compare the present work with Sugavanam *et al.*, the local velocity gradient at the heated strip was determined from detailed velocity distribution data given by Shah and London [25]. The comparison is shown in Fig. 2 in the form of spatial average Nusselt number vs the distance between the flow entrance and the leading edge of the heated strip (at $x = 0$ the heated strip is located at the flow entrance). The case shown is for $D/a = 1$, $D_H = 1$ cm, $Re = 1260$ and $k_f/k_s = 10$, so that the fluid-side heat transfer is very important in describing the conjugate heat transfer. The agreement is good when the heated strip is near the flow entrance and the agreement improves as the distance from the entrance increases; the values agree within 1% for $x/(D_H Re) > 0.005$. Here D_H is the hydraulic diameter and Re is the Reynolds number based on hydraulic diameter. This comparison shows that the linear velocity model is a useful approximation in a developing flow if the thermal effects are dominated by the flow field directly above the heated strip ($\Lambda > 1$) and if the velocity gradient is not changing too rapidly. The linear velocity distribution is exactly correct for fully developed fluid flow ($\beta \neq \beta(x)$) over a small heated strip, because the thermal boundary layer will be limited to the linear region of the hydrodynamic boundary layer.

3. RESULTS, $1 < \Lambda < 100$

The computational efficiency of the SE method has made it possible to explore a wide range of conjugate heat transfer behaviors by varying the conjugate Peclet number Λ and geometric ratio D/a. Typical Λ-values that arise in actual linear flow are given in Table 1 for Blasius flow over a flat plate with a heated region of length $2a = 20$ mm located at $x = 100$ mm and for air and water flow over three different electronic materials. The range of values $1 < \Lambda < 100$ covers a wide variety of conjugate geometries. Because Λ contains the velocity gradient to the 1/3 power, a hundred-fold variation in Λ represents a million-fold variation in fluid velocity gradient.

3.1. *Distributions on the interface*

Figure 3 shows the dimensionless interface temperature vs x/a geometry $D/a = 10$ for three cases $\Lambda = 1$, 10 and 100. Here 64 surface elements (16 on the heated region) were used to give a smooth distribution. The heated region is located at $-1 \leqslant x/a \leqslant 1$ and as expected the temperature is highest there. As parameter Λ increases the temperature decreases everywhere, and the upstream temperature is most strongly affected, so that at $\Lambda = 100$ the temperature is essentially zero upstream of the heated region. The shape of the temperature curve at

Table 1. Typical Λ values for laminar flow (fluid) over a flat plate (solid) for several fluid–solid combinations

Fluid/solid	k_f/k_s	Pr	Re_x	$\frac{\beta a^2}{\alpha_f}$	$(k_s/k_f)^2\Lambda$	Λ
Air/silicon	0.000178	0.69	10^4	$2.28(10^3)$	$7.39(10^4)$	0.00234
			10^6	$2.28(10^6)$	$7.39(10^5)$	0.0234
Air/alumina (96%)	0.001257	0.69	10^4	$2.28(10^3)$	$1.04(10^4)$	0.0165
			10^6	$2.28(10^6)$	$1.04(10^5)$	0.165
Air/epoxy fiberglass (FR-4)	0.11	0.69	10^4	$2.28(10^3)$	$1.20(10^2)$	1.45
			10^6	$2.28(10^6)$	$1.20(10^3)$	14.5
Water/silicon	0.00406	6.7	10^4	$2.22(10^4)$	$6.92(10^3)$	0.114
			10^6	$2.22(10^7)$	$6.92(10^4)$	1.14
Water/alumina (96%)	0.0287	6.7	10^4	$2.22(10^4)$	980.0	0.807
			10^6	$2.22(10^7)$	9800.0	8.07
Water/epoxy fiberglass (FR-4)	2.51	6.7	10^4	$2.22(10^4)$	11.2	70.5
			10^6	$2.22(10^7)$	112.0	705.0

NOTE: $\tau = 1/2\rho V_\infty^2 \cdot C_{fx}$

$C_{fx} = 0.664/\sqrt{Re_x}$

$x/a = 10$.

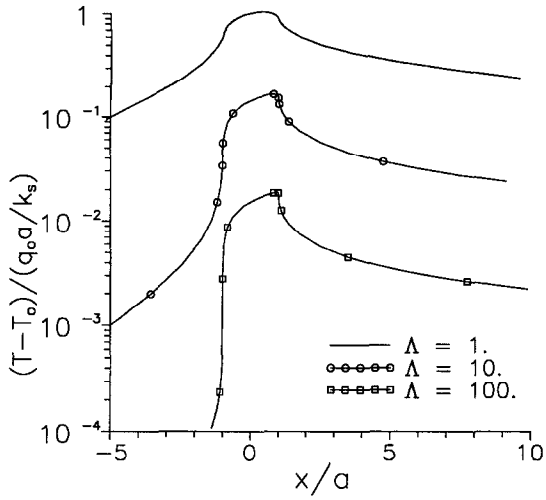

Fig. 3. Temperature along the fluid–solid interface; the heat source is located on $(-1 < x/a < 1)$.

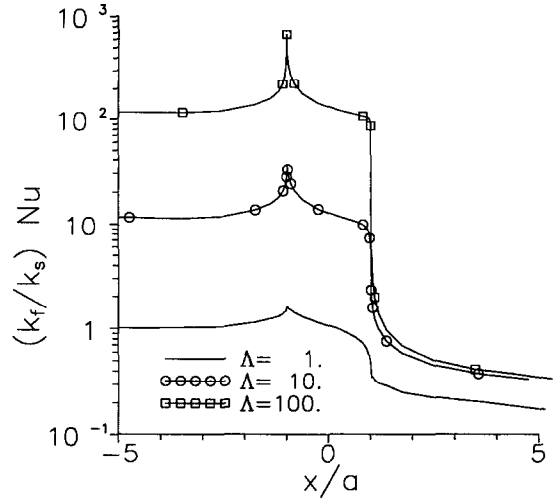

Fig. 5. Modified Nusselt number along the fluid–solid interface.

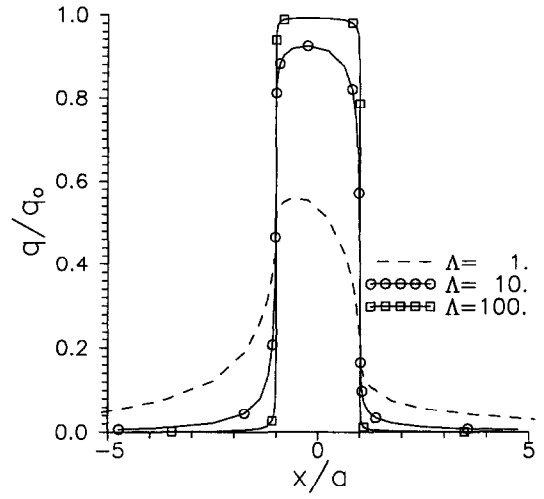

Fig. 4. Heat flux to the fluid along the fluid–solid interface.

$\Lambda = 100$ is the same as that predicted by a fluid alone heated uniformly over a small heated region and insulated elsewhere (see for example ref. [26] page 363). Slightly downstream of the heated region the temperature decays at the same rate for every Λ-value; this behavior was also observed experimentally by Ortega *et al.* [22].

Figure 4 shows the normalized heat flux entering the fluid along the interface for the same conditions as Fig. 3. This problem involves a split in heat at the heated region; some of the introduced heat goes directly to the fluid and some goes directly to the solid. The heat flux distribution is strongly local to the heated region, and outside the heated region the heat flux is larger upstream compared to downstream. As Λ increases the (normalized) fluid heat flux approaches 1.0 on the heated region, which means that most of the heat flows directly to the fluid. All of the introduced heat eventually finds its way into the fluid because the solid is insulated at $y_s = D$. Consequently the integral of the heat flux q_f over the interface is equal to the introduced heat, $\int q_f \, dx = 2a \cdot q_0$.

Together the temperature and heat flux distributions completely characterize the heat transfer at the interface and the Nusselt number is derived from these. Figure 5 shows the modified Nusselt number $N_u^*(x)$ vs x^+ for the same conditions as Figs. 3 and 4. In Fig. 5 the three curves at $\Lambda = 1$, 10 and 100 have different average values; however, all three curves have a very similar shape. The fact that the shape of the N_u^* curve is similar across a wide range of Λ-values indicates that the modified Nusselt number distribution does not show the fluid-dominated behavior at large Λ-values. In contrast the temperature and heat flux curves (Figs. 3 and 4) change shape when the fluid dominates the heat transfer. The point of this discussion is that a study of the Nusselt number, by itself, is not sufficient to characterize when conjugate heat transfer is dominated by the fluid.

Far upstream of the heated strip the N_u^* value is constant since in the present study the velocity field is everywhere fully developed and the solid extends infinitely far upstream; there is no abrupt 'leading edge' in the computational domain. In a study of entrance flow, Sugavanam *et al.* [19] show that N_u is also constant in a region upstream of the heated strip, however at the leading edge of the plate the N_u values show a precipitous peak. This is expected from convection theory which predicts that the heat transfer coefficient becomes infinite where a thermal boundary layer begins abruptly, such as at the leading edge of a solid plate.

3.2. *Spatial averages on the heated strip*

The spatial average modified Nusselt number on the heated region is plotted in Fig. 6 in the form $\overline{N_u^*}$

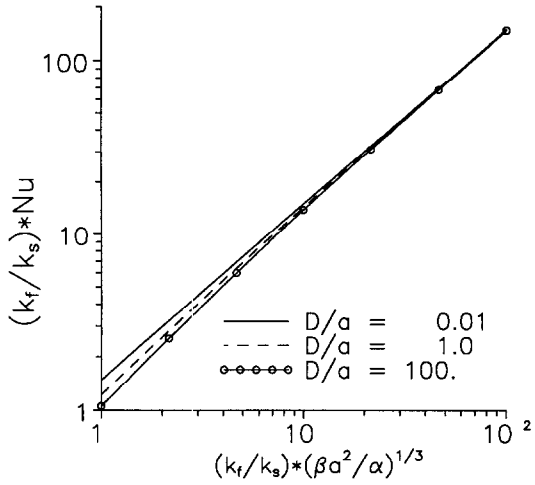

Fig. 6. Spatial average modified Nusselt number versus conjugate Peclet number for $D/a = 0.01$, 1.0 and 100.

vs Λ for several D/a values. At larger values of Λ all the geometries give the same limiting behavior of flow-dominated heat transfer described by a straight line

$$\overline{N_u^*} = C\Lambda \tag{19}$$

where C is a constant. The above equation may be multiplied by k_s/k_f to give

$$\overline{N_u} = CP_e^{1/3}. \tag{20}$$

This proportionality between the ordinary Nusselt number $\overline{N_u}$ and the one-third power of Peclet number was first shown in 1954 by Liepmann and Skinner [27] by a dimensional argument. The value of the proportionality constant C can be derived from fluid-only theory [28] by taking the spatial average of the heat transfer coefficient on a uniformly heated region in a shear flow: $C = (3/2)^{1/3}\Gamma(2/3) = 1.550$ where Γ is the gamma function.

In Fig. 7 the spatial-average heat flux from the heated strip to the fluid $\overline{q_f^+}$ is presented vs Λ. The heat flux depends strongly on D/a at small values of Λ, and as Λ increases the values of $\overline{q_f^+}$ all approach the value unity. There are at least two ways to look at this large-Λ limit. If Λ becomes large because the fluid flow becomes large, then the fluid-side heat transfer coefficient is large and most of the heat goes directly to the fluid flow. If Λ increases because the conductivity ratio k_f/k_s increases, then the effect of the solid decreases and a decreasing fraction of the heat goes directly to the solid. If the effect of the solid disappears then the effect of solid thickness D/a must also disappear.

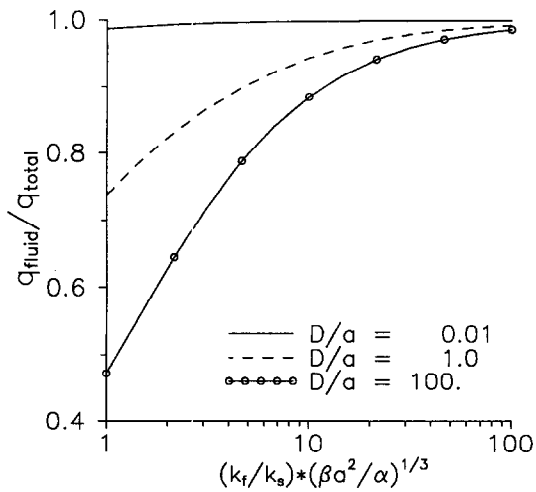

Fig. 7. Spatial-average heat flux to the fluid vs conjugate Peclet number for $D/a = 0.01$, 1.0 and 100.

Anderson [15] defines a dimensionless parameter for conjugate problems to predict when convection-only theory may be used to predict the temperature on the interface. Anderson defines a Biot number by

$$B_i = \frac{\bar{h}(2a)}{k_s}\frac{(2a)}{D} = \overline{N_u^*}\frac{2a}{D}$$

which is the ratio of the resistance to conduction along the solid to the resistance to convection from the heated strip. Anderson states that for $B_i > 1$ the temperature may be calculated with reasonable approximation by fluid-only theory, and for $B_i < 1$ conjugate analysis is required. Present research indicates that the use of fluid-only theory at $B_i = 1$ is least accurate at $D/a = 1$ and the accuracy improves as D/a moves away from 1. A criterion from the present research for uniform accuracy at various D/a values may be based on parameter Λ: spatial average temperature predicted by fluid-only theory will be accurate within 5% for $\Lambda > 10$.

3.3. *Correlations*

A correlation for $\overline{N_u^*}$ that matches Fig. 6 within 4% everywhere for $0.01 \leqslant D/a \leqslant 100$ and $1 \leqslant \Lambda \leqslant 100$ is given by

$$\overline{N_u^*} = 1.5\Lambda - 1.3\left(\frac{D/a}{D/a+0.6}\right)\left(\frac{\Lambda}{\Lambda+2.2}\right). \tag{21}$$

A correlation for $\overline{q_f^+}$ vs Λ based on the relative size of the thermal resistance for heat transfer from the fluid and the solid that agrees with Fig. 7 within 4% is given by

$$\overline{q_f^+} = \frac{\Lambda}{\Lambda + 1.2\left(\dfrac{D/a}{D/a+1.9}\right)}. \tag{22}$$

Temperature values have been omitted due to space limitations. The local temperature is related to heat flux and Nusselt number exactly by $T^+(x) = q_f^+(x)/N_u^*(x)$. However, the spatial-average temperature on the heated region can be calculated approximately from the $\overline{N_u^*}$ and $\overline{q_f^+}$ values given above by $\overline{T^+} = \overline{q_f^+}/\overline{N_u^*}$. This expression is approximate

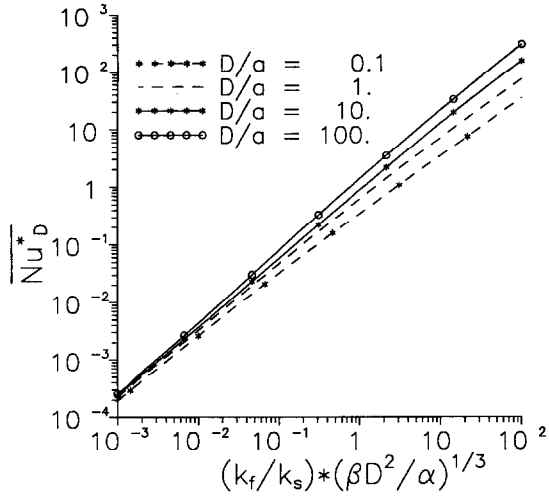

Fig. 8. Spatial average modified Nusselt number based on length scale D, $\overline{N_u^*}_D = \bar{h}D/k_s$, vs conjugate Peclet number based on length scale D.

because the integral of a quotient is different from the quotient of integrals.

4. RESULTS, $10^{-3} < \Lambda < 100$

Figure 8 shows the dimensionless heat transfer coefficient normalized by length scale D vs the conjugate Peclet number normalized by length D. With length scale D the appropriate modified Nusselt number is given by $\overline{N_u^*} = hD/k_s$, and the appropriate conjugate Peclet number is $\Lambda_D \equiv (k_f/k_s)(\beta D^2/\alpha_f)^{1/3}$. In Fig. 8 all of the different D/a curves converge towards one curve at small values of Λ_D. In this regime, solid thickness D is better for normalizing the heat transfer instead of heated strip size 'a'. This can be understood by considering that Λ_D is proportional to fluid velocity gradient to the one-third power, and therefore small Λ_D represents small fluid heat transfer coefficient. Other things being equal, as the heat transfer coefficient becomes smaller the temperature on the heated strip increases, more of the introduced heat flows directly to the solid, and a larger surface area is needed to transfer the heat to the fluid. Recall that all of the heat must eventually find its way to the fluid. Eventually the warmed region of the fluid–solid interface becomes much larger than the heated strip, and the size of the heated strip 'a' must have a decreasing influence on the results as Λ_D decreases.

In the special case for which the solid is of finite extent upstream of the heated strip (not studied in this paper), in the limit as $\Lambda_D \to 0$ the plate becomes isothermal. For the finite-length plate the limit $\Lambda_D \to 0$ is equivalent to $k_s \to \infty$ and the solid-side thermal resistance will be small compared to the fluid-side thermal resistance (small Biot number). Under these circumstances the finite-length plate is similar to the geometry of Luikov [2] for which the Brun number given by equation (15) may be used with $x = L$, where L is the length of the plate.

5. AXIAL HEAT CONDUCTION IN THE FLUID

In this section the assumption of neglecting the fluid axial heat conduction is addressed. Several researchers have included the axial conduction of heat in the fluid for conjugate heat transfer calculations [16, 29–32] and all have indicated that axial heat conduction in the fluid is negligible if the flow is large (large Pe) or if the solid thermal conductivity is much larger than that of the fluid (large k_s/k_f).

In the Appendix an integral energy equation is developed that includes parameter $(k_s/k_f)^2\Lambda$. The integral energy equation suggests that when parameter $(k_s/k_f)^2\Lambda$ is large the axial conduction in the fluid may be neglected.

Data from the literature has been used to show that large values of parameter $(k_s/k_f)^2\Lambda$ are correlated with cases for which the fluid axial conduction may be neglected. Table 2 contains a comparison of the spatial average Nusselt number for conjugate heat transfer calculations that include axial fluid conduction [32] with calculations that do not [23, 33]. The last column in Table 2 contains the percent error caused by neglecting axial fluid conduction. The error has a well-defined trend that falls along a straight line on a log-log plot (not shown). This suggests that a power-law fit to the data is appropriate, and a best fit of the error data has the form

$$y = 0.0595[(k_s/k_f)^2\Lambda]^{-0.623}$$

where y is the error (percent). This curve fit suggests that the error associated with neglecting the fluid axial conduction in conjugate calculations is less than 1% for $(k_s/k_f)^2\Lambda \geqslant 18$. This condition is satisfied for many engineering flows, especially air flows. Refer to Table 1 which contains values of parameter $(k_s/k_f)^2\Lambda$ in laminar flow for several fluid–solid combinations. The only case in Table 1 for which $(k_s/k_f)^2\Lambda < 18$ is for low speed water flow over epoxy-plexiglas.

6. SUMMARY

In this paper conjugate heat transfer results have been presented in a compact manner for a wide range of conjugate Peclet number $\Lambda = (k_f/k_s)P_e^{1/3}$ and solid thickness D. For large values of Λ, fluid-flow behavior dominates and the appropriate length scale is the size of the heated strip; for small values of Λ the appropriate length scale is the thickness of the solid. Simple correlations for the heat transfer coefficient and for the fluid heat flux are suggested as predictive tools for conjugate heat transfer over a wide range of fluid flow, thermal conductivity, and solid thickness; one application is cooling of electronic components. Although the results presented are based on a fully-developed linear velocity profile, the Nusselt number

Table 2. Percent error in Nusselt number caused by neglecting fluid axial conduction, tabulated vs parameter $(k_s/k_f)^2\Lambda$ for $D/a = \infty$

$(k_s/k_f)^2\Lambda$	k_s/k_f	b/a	Ref. [32]	Ref. [23]	Ref. [33]	% difference
79.4	50	1	108.0	—	108.55	0.50
200	50	1	112.3	—	112.72	0.37
31.75	20	1	45.55	—	45.07	1.06
50.40	20	1	46.91	—	46.64	0.58
17.46	11	5	14.83	—	14.71	0.82
27.72	11	5	16.27	—	16.14	0.77
36.32	11	5	17.43	—	17.32	0.61
6.51	4.1	8	6.57	—	6.44	2.01
15.87	10	∞	8.79	8.69	—	1.20
25.20	10	∞	10.98	10.49	—	0.83
33.07	10	∞	11.94	11.87	—	0.62
40	10	∞	13.10	13.03	—	0.53
7.83	5	∞	5.94	5.82	—	1.90
12.60	5	∞	7.44	7.35	—	1.20
16.51	5	∞	8.63	8.55	—	0.93
20.00	5	∞	9.66	9.59	—	0.71

Here b/a is the width/length of the rectangular heated region, $b/a = \infty$ is the 2-D strip

results are accurate in developing laminar flows with errors of less than 1% for $x/(D_H Re) > 0.005$. Also, a new combined parameter $(k_s/k_f)^2\Lambda$ is associated with fluid axial heat conduction; fluid axial conduction can be neglected in conjugate heat transfer within 1% error when $(k_s/k_f)^2\Lambda > 18$.

REFERENCES

1. Perelman, T. L., On conjugated problems of heat transfer. *International Journal of Heat & Mass Transfer*, 1961, **3**, 293–303.
2. Luikov, A. V., Conjugate convective heat transfer problems. *International Journal of Heat & Mass Transfer*, 1974, **17**, 257–265.
3. Sparrow, E. M. and Chyu, M. K., Conjugate forced convection–conduction analysis of heat transfer in a plate fin. *Journal of Heat Transfer*, 1982, **104**, 204–206.
4. Wijeysundera, N. E., Laminar forced convection in circular and flat ducts with wall axial conduction and external convection. *International Journal of Heat & Mass Transfer*, 1986, **29**, 797–807.
5. Cole, K. D. and Beck, J. V., Conjugated heat transfer from a strip heater with the unsteady surface element method. *IAAA J. of Thermophysics and Heat Transfer*, 1987, **1**, 348–354.
6. Lee, W. C. and Ju, Y. H., Conjugate Leveque solution for Newtonian fluid in a parallel plate channel. *International Journal of Heat & Mass Transfer*, 1986, **29**, 941–947.
7. Rizk, T. A., Kleinstreuer, C. and Ozisik, M. N., Analytic solution to the conjugate heat transfer problem of flow past a heated block. *International Journal of Heat & Mass Transfer*, 1992, **35**, 1519–1525.
8. Pozzi, A. and Lupo, M., The coupling of conduction with forced convection over a flat plate. *International Journal of Heat & Mass Transfer*, 1989, **32**, 1207–1214.
9. Pop, I. and Ingham, D. B., A note on conjugate forced convection boundary-layer flow past a flat plate. *International Journal Heat & Mass Transfer*, 1993, **36**, 3873–3876.
10. Davis, E. J. and Gill, W. N., The effects of axial conduction in the wall on heat transfer with laminar flow. *International Journal of Heat & Mass Transfer*, 1970, **13**, 459–470.
11. Mori, S., Shinke, T., Sakakibara, M. and Tanimoto, A., Steady heat transfer to laminar flow between parallel plates with conduction in wall. *Heat Transfer, Japanese Research*, 1976, **5**, 17–25.
12. Lin, Y. K. and Chow, L. C., Effects of wall conduction on heat transfer for turbulent flow in a circular tube. *Journal of Heat Transfer*, 1984, **106**, 597–604.
13. Cole, K. D. and Beck, J. V., Conjugated heat transfer from a hot-film probe for transient air flow. *Journal of Heat Transfer*, 1988, **110**, 290–296.
14. Culham, J. R., Lemczyk, T. F., Lee, S. and Yovanovich, M. M., META–a conjugate heat transfer model for air cooling of circuit boards with arbitrarily located heat sources. *Heat Transfer in Electronic Equipment*. HTD-Vol. 171, ASME, New York, 1991.
15. Anderson, A. M., Decoupling convective and conductive heat transfer using the adiabatic heat transfer coefficient. *Journal of Electronic Packaging*, 1994, **116**, 310–316.
16. Ramadhyani, S., Moffatt, D. F. and Incopera, F. P., Conjugate heat transfer from small isothermal heat sources embedded in a large substrate. *International Journal of Heat & Mass Transfer*, 1985, **28**, 1945–1952.
17. Incropera, F. P., Kerby, J. S., Moffatt, D. F. and Ramadhyani, S., Convection heat transfer from discrete heat sources in a rectangular channel. *International Journal of Heat & Mass Transfer*, 1986, **29**, 1051–1058.
18. Prasad, B. V. S. S. S. and Dey Sarkar, S., Conjugate laminar forced convection from a flat plate with imposed pressure gradient. *Journal of Heat Transfer*, 1993, **115**, 469–472.
19. Sugavanam, R., Ortega, A. and Choi, C. Y., A numerical investigation of conjugate heat transfer from a flush heat source on a conductive board in laminar channel flow. *International Journal of Heat & Mass Transfer*, 1995, **38**, 2969–2984.
20. Ortega, A., Conjugate heat transfer in forced air cooling of electronic components. In *Air Cooling Technology for Electronic Equipment*, ed. S. J. Kim and S. W. Lee, Chap. 4. CRC Press, Cleveland, OH, 1996.
21. Liu, T., Campbell, B. T. and Sullivan, J. P., Surface temperature of a hot film on a wall in shear flow. *International Journal of Heat & Mass Transfer*, 1994, **37**, 2309–2814.
22. Ortega, A., Wirth, U. S. and Kim, S. J., Conjugate forced convection from a discrete heat source on a plane conducting surface: a benchmark experiment. In HTD-292, *Heat Transfer in Electronic Systems*. ASME, New York, 1994.

23. Cole, K. D., Conjugated heat transfer with the unsteady surface element method. Ph.D. thesis, Michigan State University, East Lansing, MI, 1986.
24. Beck, J. V., Cole, K. D., Haji-Sheikh, A. and Litkouhi, B., *Heat Conduction using Green's Functions*, Chap. 4. Hemisphere, New York, 1992.
25. Shah, R. K. and London, A. L., *Laminar Forced Convection in Ducts*. Academic Press, New York, 1978, p. 162.
26. Bird, R. B., Stewart, W. E. and Lightfoot, E. N., *Transport Phenomena*. Wiley, New York, 1960, pp. 363–364.
27. Liepmann, H. W. and Skinner, G. T., Shearing stress measurements by use of a heated element. NACA Technical note 3268, 1954.
28. Wang, C. Y., Shear flow over a wall with variable temperature. *Journal of Heat Transfer*, 1991, **113**, 496–498.
29. Faghri, M. and Sparrow, E. M., Simultaneous wall and fluid axial conduction in laminar pipe-flow heat transfer. *Journal of Heat Transfer*, 1980, **102**, 58–63.
30. Soliman, H. M., Analysis of low-Peclet heat transfer during slug flow in tubes with axial wall conduction. *Journal of Heat Transfer*, 1984, **106**, 782–788.
31. Zebib, A. and Wo, Y. K., A two-dimensional conjugate heat transfer model for forced air cooling of an electronic device. *Journal of Electronic Packaging*, 1989, **111**, 41–45.
32. Kalumuck, K. M., A theory for the performance of hot-film shear stress sensors. Ph.D. thesis, MIT, Cambridge, MA, 1983.
33. Liang, P. W., Unsteady shear stress measurements with heated films—analysis and experiment. Ph.D. thesis, University of Nebraska, Lincoln, NE, 1992.
34. Murphy, G., *Similitude in Engineering*. Ronald Press, New York, 1950, p. 62.

APPENDIX—COMBINED PARAMETER FOR FLUID AXIAL CONDUCTION

The fluid axial conduction may often be safely neglected in conjugate heat transfer because either the fluid flow is rapid, described by a large enough Peclet number Pe, or because the thermal conductivity of the solid is much larger than that of the fluid, described by large k_s/k_f. These separate dimensionless parameters Pe and k_s/k_f arise from the convection-only theory and from conduction-only theory, respectively. In this Appendix a combined parameter $(k_s/k_f)^2\Lambda$ is derived, that determines when the fluid axial conduction term can be neglected.

Integral energy equation

An integral energy analysis will be carried out on a control volume that encompasses both the solid and the fluid. The control volume has thickness dx in the streamwise direction and height that is large enough to include the entire thickness of the solid and the entire thermal boundary layer in the fluid. The control volume is shown in Fig. A1.

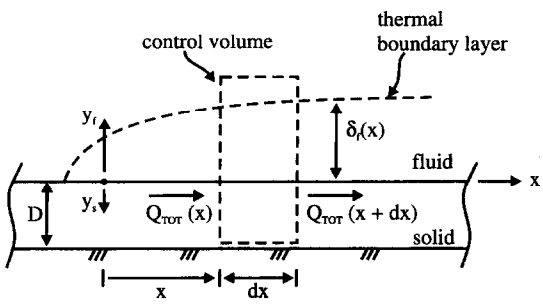

Fig. A1. Control volume that encompasses the solid and the thermal boundary layer.

A steady energy balance on the control volume involves three terms: the heat passing through the left-hand face, the heat passing through the right-hand face, and any heat introduced at the fluid–solid interface by the heated strip. The energy balance on the control volume is

$$Q_{tot}(x) - Q_{tot}(x+dx) + q(x)\cdot w\cdot dx = 0. \tag{A1}$$

Here Q_{tot} represent the total x-direction transport of heat (W) through the control volume caused by all mechanisms in both the solid and the fluid; $q(x)$ is the heat flux (W m^{-2}) introduced by the heated strip; and, w is the out-of-plane width of the control volume. There is no y-direction transport of heat across the control volume surface because the bottom of the solid is insulated and the top of the control volume extends beyond the thermal boundary layer. Next divide the above equation by $w\cdot dx$ and take the limit as $dx \to 0$ to find a differential equation for the x-direction transport of heat:

$$-\frac{1}{w}\frac{dQ_{tot}(x)}{dx} + q(x) = 0. \tag{A2}$$

This equation indicates that the derivative of the x-direction transport is proportional to the heat introduced by the heated strip.

There are three mechanisms that contribute to the total x-direction transport of heat in conjugate heat transfer: the x-direction conduction in the solid Q_s; the x-direction conduction in the fluid Q_f (the axial fluid conduction term); and, the velocity-based convection in the fluid Q_{conv}. That is,

$$Q_{tot}(x) = Q_s(x) + Q_f(x) + Q_{conv}(x). \tag{A3}$$

The relative size of these transport terms will determine whether or not $Q_f(x)$ may be neglected. The Q-terms may be stated in the form of temperature by an integral description over the left-hand face of the control volume as follows:

$$Q_s(x) = \int_0^D \left(-k_s\frac{\partial T_s}{\partial x}\right) w\, dy_s \tag{A4}$$

$$Q_f(x) = \int_0^{\delta_f} \left(-k_f\frac{\partial T_f}{\partial x}\right) w\, dy_f \tag{A5}$$

$$Q_{conv}(x) = \int_0^{\delta_f} (\rho_f c_f(\beta y_f) T_f) w\, dy_f. \tag{A6}$$

Here δ_f is the local thickness of the thermal boundary layer in the fluid. Next these integral terms will be made dimensionless with the variables given in equation (7):

$$\frac{Q_s(x)}{q_0 a w} = \int_0^{D/a} \left(-\frac{\partial T_s^+}{\partial x^+}\right) dy_s^+$$

$$\frac{Q_f(x)}{q_0 a w} = \frac{1}{(k_f/k_s)^2\Lambda}\int_0^{(\delta_f/a)P_e^{1/3}} \left(-\frac{\partial T^+}{\partial x^+}\right) dy_f^+$$

$$\frac{Q_{conv}(x)}{q_0 a w} = \Lambda\int_0^{(\delta_f/a)P_e^{1/3}} (y_f^+ T_f^+)\, dy_f^+. \tag{A7}$$

In the above integrals the dimensionless length in the y-direction is $y_s^+ = y_s/a$ in the solid and $y_f^+ = (y_f/a)P_e^{1/3}$ in the fluid. These distinct length scales for the fluid and the solid have previously been shown to be useful for the conjugate heat transfer problem. In the above expressions, because the integral terms have been made dimensionless, the relative size of each x-direction transport term is controlled by the coefficient in front of each integral. The fluid convection term, Q_{conv}^+, has coefficient $\Lambda = (k_f/k_s)P_e^{1/3}$, the conjugate Peclet number for shear flow. Fluid convection dominates when $\Lambda > 10$ as shown in Fig. 6. The fluid axial conduction term $Q_f(x)$ and the solid conduction term $Q_s(x)$ will be of the same order of magnitude if parameter $(k_s/k_f)^2\Lambda$ is of order

unity. The fluid conduction term can be neglected next to the solid conduction term if parameter $(k_s/k_f)^2\Lambda$ is above a threshold value; an estimate of the threshold value is given in the body of the paper.

Buckingham–Pi theorem

The combined parameters discussed in this paper represent an alternative *form* of the dimensionless parameters, however the *number* of dimensionless parameters is fixed by the Buckingham–Pi theorem [34]. Briefly stated, the Buckingham–Pi theorem gives the number of dimensionless parameters, or 'Pi groups', as $n-b$ where n is the total number of quantities involved and b is the number of basic dimensions involved. The only restrictions placed upon the Pi-groups are that they be dimensionless and that they be linearly independent.

An examination of equations (1)–(6), indicates that the temperature depends on the following unit-bearing quantities:

$$T = T(x, y_s, y_f, \beta, \alpha_f, k_f, k_s, D, a, q_0). \tag{A8}$$

That is, there are 11 quantities (including the temperature) whose units contain four basic dimensions (meters, seconds, Watts, and Kelvin). The Buckingham–Pi theorem gives $11-4=7$ dimensionless parameters. There are several alternative sets of seven dimensionless parameters that could be used for this problem. For example, the length scale for the parameters can be the size of the heated strip (a) or the solid thickness (D); both of these length scales are used in this paper. One traditional set or seven dimensionless parameters is given by

$$T^+ = T^+(x^+, y_s^+, y_f^+, D/a, P_e, (k_s/k_f)). \tag{A9}$$

The present research suggests that a useful set of parameters is given by

$$T^+ = T^+(x^+, y_s^+, y_f^+, D/a, \Lambda, (k_s/k_f)^2\Lambda). \tag{A10}$$

Note that the last two parameters are linearly independent and they can be obtained by a product of powers of traditional parameters Pe and (k_s/k_f). The important benefit of this new set of parameters, and the central result of this Appendix, is that parameter $(k_s/k_f)^2\Lambda$ drops out of the dimensionless governing equations when the fluid axial conduction is negligible. An integral energy equation has been used to demonstrate this; however, the same conclusion can be drawn from the differential equations in dimensionless form.

Summary

In this Appendix a new dimensionless parameter associated with fluid axial conduction of heat has been identified from an integral energy equation that encompasses both the solid and the fluid. The new parameter combines the expected trends for the Peclet number Pe and the conductivity ratio (k_s/k_f) into a single parameter $(k_s/k_f)^2\Lambda$ for determining when the fluid axial conduction may be neglected. The new parameter is a member of an equivalent set of dimensionless parameters allowed under the Buckingham–Pi theorem.